

# Estimation of bone Calcium-to-Phosphorous mass ratio using dual-energy nonlinear polynomial functions

P Sotiropoulou<sup>1</sup>, V Koukou<sup>1</sup>, N Martini<sup>1</sup>, C Michail<sup>2</sup>, E Kounadi<sup>3</sup>, I Kandarakis<sup>2</sup>,  
G Nikiforidis<sup>1</sup> and G Fountos<sup>2</sup>

<sup>1</sup>Department of Medical Physics, Medical School University of Patras, 265 00 Patras, Greece

<sup>2</sup>Department of Medical Instruments Technology, Technological Educational Institution of Athens, 122 10 Athens, Greece

E-mail: gfoun@teiath.gr

**Abstract:** In this study an analytical approximation of dual-energy inverse functions is presented for the estimation of the calcium-to-phosphorous (Ca/P) mass ratio, which is a crucial parameter in bone health. Bone quality could be examined by the X-ray dual-energy method (XDEM), in terms of bone tissue material properties. Low- and high-energy, log-intensity measurements were combined by using a nonlinear function, to cancel out the soft tissue structures and generate the dual energy bone Ca/P mass ratio. The dual-energy simulated data were obtained using variable Ca and PO<sub>4</sub> thicknesses on a fixed total tissue thickness. The XDEM simulations were based on a bone phantom. Inverse fitting functions with least-squares estimation were used to obtain the fitting coefficients and to calculate the thickness of each material. The examined inverse mapping functions were linear, quadratic, and cubic. For every thickness, the nonlinear quadratic function provided the optimal fitting accuracy while requiring relative few terms. The dual-energy method, simulated in this work could be used to quantify bone Ca/P mass ratio with photon-counting detectors.

## 1. Introduction

Crystal structure and chemical composition of biological apatite reflect their physiological function as a mechanical support, which is very important to the skeletal system, storage of mineral, and storage of chemical energy. Alterations in the bone quality can be attributable to disease-related structural and chemical changes. Due to the complexity of bone, various methods have been used to measure bone tissue properties [1]. The relative content of calcium (Ca) and phosphorus (P) regulates the mineral homeostasis and bone metabolism [2]. Since variations in the concentrations of either Ca or P are not necessarily in mutual association, changes of the Ca/P ratio are crucial for the valuation of bone health. The Ca/P bone ratio in cases of diseases such as osteogenesis imperfecta or osteoporosis is systematically lower than that derived from normal bone samples [3,4]. Consequently, the estimation of the Ca/P ratio as a bone quality index may add valuable information regarding bone mineralization state and bone diseases [5,6,7,8,9].

In this study an analytical approximation of dual energy inverse functions is presented for the estimation of Calcium-to-Phosphorous (Ca/P) mass ratio. An X-ray dual energy (XRDE) method is used to provide the tissue materials attenuation data in order to estimate the bone quality index. The functional forms of inverse functions that have been investigated are the linear, quadratic, and cubic. Inverse fitting functions with the least-squares estimation were used to obtain fitting coefficients and calculate the thickness of each material.



## 2. Materials and Methods

### 2.1. Theory

The theory, upon which the *in vivo* estimation of skeletal Ca/P mass ratio was based, described firstly by Fountos et al [5]. The Ca/P mass ratio is obtained assuming a three-component system: Ca, PO<sub>4</sub> and water. Using the dual energy formalism, the water (soft tissue) is cancel out and the two unknown parameters are the calcium thickness ( $t_{Ca}$ ) and the phosphate thickness ( $t_{PO_4}$ ). The log-intensity function,  $Y(t_{Ca}, t_{PO_4})$ , defined as the logarithm of the ratio of the reference intensity ( $I_w$ ) to the bone intensity ( $I_b$ ), can be written as [7]

$$Y_i(t_{Ca}, t_{PO_4}) = \ln(I_{w,E_i} / I_{b,E_i}), \quad i = \ell, h \quad (1)$$

where,  $I_{o,E_\ell}$  and  $I_{o,E_h}$  are the unattenuated low- and high-energy intensity per unit energy (photons/cm<sup>2</sup>keV) at the detector input.

The low- and high-energy log-intensity values are made independently by using X-ray beams of different spectra. The goal of the presented dual energy Ca/P determination is to invert the obtained log-intensity functions,  $Y_i(t_{Ca}, t_{PO_4})$ , into Ca thickness,  $t_{Ca}(Y_\ell, Y_h)$  and PO<sub>4</sub> thickness,  $t_{PO_4}(Y_\ell, Y_h)$ . The inverse functions are nonlinear due to the polyenergetic spectra and can be approximated by surfaces of second or third order, in three dimensions [10,11]. The functional forms of inverse functions that have been investigated [10,11] for each thickness are linear, quadratic and cubic functions.

### 2.2. Incident spectra

Experimental measurements of incident spectra were carried out using an XRDE system [7] incorporating a Cadmium Telluride (CdTe) photon counting detector [12,13,14,15]. The 100kVp energy spectrum from the Tungsten anode, after 0.88 g/cm<sup>2</sup> Ce filtration resulted in two energy bands with mean energies of 38keV (low-energy spectrum, LE) and 86keV (high-energy spectrum, HE).

### 2.3. Simulated calibration data

Simulations of scale phantoms were performed for investigation of the inverse functions and the determination of polynomial's coefficients. Software phantoms consisted of water and hydroxyapatite were used, to simulate a finger of 2.8cm total thickness. The simulated calibration data were obtained from seven thicknesses of each component, ranging from 0.0210-0.0438cm and 0.1260-0.1488cm for Ca and PO<sub>4</sub> thicknesses, respectively. Thus 49 calibration points were acquired. The reference intensity ( $I_{w,E_i}$ ) and the unattenuated intensity level ( $I_{o,E_i}$ ) were measured considering Poisson noise and source stability. The attenuated intensities,  $I_{b,E_i}$ , were estimated from the software phantoms. To estimate the fitting accuracy of the different inverse functions the residuals of the fit were determined.

## 3. Results and Discussion

The calculated low-energy and high-energy log-intensity values are plotted in Figure 1. The range of the log-intensity values are 0.28 to 0.46 and 0.07 to 0.10 for the low- and high-energy, respectively. The maximum log-intensity values are attainable in highest thicknesses where there is the maximum attenuation. In LE the modulation of log-intensity values is greater than in HE, due to higher attenuation of the photons in low energies.

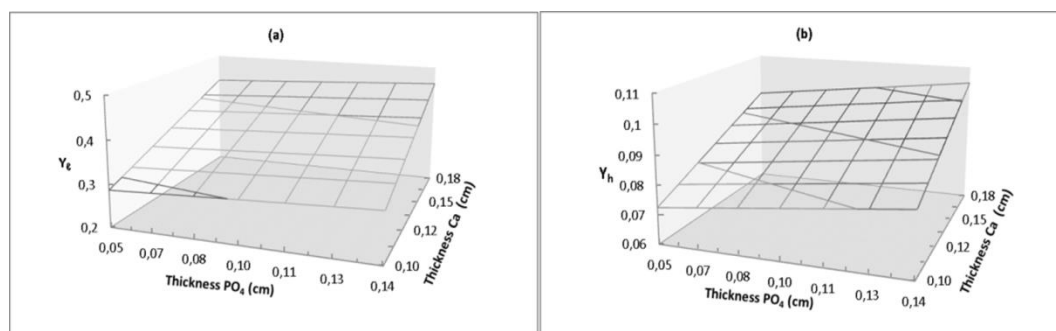


**Figure 1.** The calibration (a) LE and (b) HE log-intensity values, as a function of the  $Ca$  and  $PO_4$  thickness, used to compute the various inverse functions.

The thickness of each material was fitted separately using a nonlinear least squares analysis. The median,  $\delta_{med}$ , the standard deviation,  $\delta_{rms}$ , and the maximum absolute deviation,  $\delta_{max}$  of the residual values for each of the inverse function are presented in Table 1.

**Table 1.** The median, standard deviation and maximum absolute deviation of the residual values from the fit to  $Ca$  and  $PO_4$  thicknesses of the simulated data.

Functional models	$Ca$ thickness (cm)			$PO_4$ thickness (cm)		
	$\delta_{med}$	$\delta_{rms}$	$\delta_{max}$	$\delta_{med}$	$\delta_{rms}$	$\delta_{max}$
Linear	$-6.6 \cdot 10^{-6}$	$2.4 \cdot 10^{-5}$	$4.9 \cdot 10^{-5}$	$-3.1 \cdot 10^{-5}$	$8.0 \cdot 10^{-5}$	$1.8 \cdot 10^{-4}$
Quadratic	$-3.4 \cdot 10^{-9}$	$1.5 \cdot 10^{-8}$	$2.7 \cdot 10^{-8}$	$4.0 \cdot 10^{-8}$	$1.3 \cdot 10^{-6}$	$3.1 \cdot 10^{-6}$
Cubic	$1.8 \cdot 10^{-10}$	$3.9 \cdot 10^{-9}$	$8.7 \cdot 10^{-9}$	$-1.2 \cdot 10^{-9}$	$2.3 \cdot 10^{-8}$	$5.1 \cdot 10^{-8}$

As it can be seen from Table 1, the linear function inadequately modeled both thicknesses. The accuracy of the cubic function, with  $\delta_{med}$  of  $1.8 \cdot 10^{-10}$  cm and  $\delta_{rms}$  of  $3.9 \cdot 10^{-9}$  cm, for  $Ca$  thickness and with  $\delta_{med}$  of  $-1.2 \cdot 10^{-9}$  cm and  $\delta_{rms}$  of  $2.3 \cdot 10^{-8}$  cm for  $PO_4$  thickness, is slightly better than the accuracy of the quadratic function. However, the quadratic function requires a smaller number of terms compared to the cubic function.

#### 4. Conclusions

A nonlinear quadratic function demonstrated high fitting accuracy, for each thickness, while requiring relative few terms. The proposed method showed that it is possible to quantify bone Ca/P mass ratio by using dual energy techniques and photon-counting detectors.

#### Acknowledgement

This research has been co-funded by the European Union (European Social Fund) and Greek national resources under the framework of the “Archimedes III: Funding of Research Groups in TEI of Athens” project of the “Education & Lifelong Learning” Operational Programme.

#### 5. References

- [1] Malluche H, Porter D and David Pienkowski 2013 *Nat. Rev. Nephro.* **11** 671
- [2] Masuyama R, Nakaya Y, Katsumata S, Kajita Y, Uehara M, Tanaka S, Sakai A, Kato S, Nakamura T and Suzuki K 2003 *J. Bone Miner. Res.* **18** 1217
- [3] Tzaphlidou M 2008 *J. Biol. Phys.* **34** 39

- [4] Kounadi E, Fountos G and Tzaphlidou M 1998 *Connect. Tissue Res.* **37** 69
- [5] Fountos G, Yasumura S and Glaros D 1997 *Med. Phys.* **24** 1303
- [6] Fountos G, Tzaphlidou M, Kounadi E and Glaros D 1999 *Appl. Radiat. Isot.* **51** 273
- [7] Sotiropoulou P, Fountos G, Martini N, Koukou V, Michail C, Kandarakis I and Nikiforidis G 2015 *Phys. Medica* doi:10.1016/j.ejmp.2015.01.019
- [8] Sotiropoulou P, Fountos G, Martini N, Koukou V, C Michail C, Valais I, Kandarakis I and Nikiforidis G 2014 X-ray spectra for bone quality assessment using energy dispersive counting and imaging detectors with dual energy method *XIII Mediterranean Conf. on Medical and Biological Engineering and Computing 2013 (Seville, Spain, 25–28 September 2013) (IFMBE Proceedings Vol 41)* ed LM Roa Romero (Springer Int.) pp. 463
- [9] Zoehrer R, Perilli E, Kuliwaba JS, Shapter NL, Fazzalari NL and Voelcker NH 2012 *Osteoporos. Int.* **23** 1297
- [10] Cardinal HN and Fenster A 1991 *Med. Phys.* **18** 867
- [11] Lemacks M, Kappadath S, Shaw C, Liu X and Whitman G 2002 *Med. Phys.* **29** 1739
- [12] Martini N, Koukou V, Michail C, Sotiropoulou P, Kalyvas N, Kandarakis I, Nikiforidis G and Fountos G *Journal of Spectroscopy* **2015** Article ID 563763
- [13] Michail C M, Spyropoulou V A, Fountos G P, Kalyvas N E, Valais I G, Kandarakis I S and Panayiotakis G S 2011 *IEEE Trans. Nucl. Sci.* **58(1)** 314
- [14] Michail CM, Fountos G P, Valais I G, Kalyvas N, Liaparinos P, Kandarakis I S, Panayiotakis G S 2011 *IEEE Trans. Nucl. Sci.* **58(5)** 2503
- [15] Seferis I E, Michail C M, Valais I G, Fountos G P, Kalyvas N I, Stromatia F, Oikonomou G, Kandarakis I S, Panayiotakis G S 2013 *Nucl. Instrum. Meth. Phys. Res. A.* **729** 307